

Estimates of Intensity, Wavelength, and Bandwidth Scaling of Brillouin Backscatter

Kent Estabrook, Judith Harte, E. M. Campbell, F. Ze,
D. W. Phillion, M. D. Rosen, and J. T. Larsen

Lawrence Livermore Laboratory, University of California, Livermore, California 94550
(Received 23 April 1980)

A simple nonlinear, one-dimensional spherical Brillouin-backscatter model adapted from kinetic simulations and Kruer's theory to a fluid code (LASNEX) is described. Laser absorption and Brillouin reflection are plotted for $0.265 \mu\text{m} < \lambda_0 < 10.6 \mu\text{m}$ and $3 \times 10^{13} \text{ W/cm}^2 < \text{laser intensity} < 3 \times 10^{16} \text{ W/cm}^2$ on gold disks (pulse length = 1 nsec) and the calculated absorption is compared with experiments. Kinetic simulations suggest methods of reducing the Brillouin backscatter, such as use of a wide bandwidth and multiline laser.

PACS numbers: 52.25.Ps, 52.65.+z

Experiments^{1,2} have demonstrated that Brillouin scattering can reflect large amounts of laser light. This paper describes simple numerical methods of modeling Brillouin scatter^{3,4} and some results of wavelength, intensity, and bandwidth scaling. We fit the data from a one-dimensional (1D), kinetic, relativistic, electromagnetic simulation code, OREMP³ to an adaptation of the Brillouin-backscatter scaling² which is made independent of zoning [Eq. (1)]. The reflection coefficient may be written as

$$R = 1 - \exp\left(-\frac{A[(v_0/v_i)^2(n/n_c)(l/\lambda_0)]}{(\omega_i/\omega_r)[1+(3T_e/ZT_e)](1-n/n_c)G_\nabla}\right) \\ = 1 - e^{-a}, \quad (1)$$

where ω_r/ω_0 = (ion acoustic frequency)/(laser frequency) = $k c_s/\omega_0$, $c_s = \{(ZT_e + 3T_i)/[m_i(1+k^2\lambda_D^2)]\}^{1/2}$, k (the ion acoustic wave number) = $2(\omega_0/c)(1-n/n_c)^{1/2}$, ω_i accounts for ion Landau damping,^{4,5} l is the zone length, n/n_c is the ratio of the electron density to the critical density, v_0 [= $eE(\text{position})/m_e\omega_0$] is the electron peak oscillatory velocity in the electric field (E) of the laser light of angular frequency ω_0 , λ_0 is the laser vacuum wavelength, I is the laser vacuum intensity in watts per square centimeter, $v_i^2 = T_e/m_e$, and G_∇ is the gradient damping term⁶ adapted from Nishikawa and Liv⁷ and Rosenbluth,⁷ which forms the dominant damping, $G_\nabla = 1 + (K_{\nabla n}' + K_{\nabla v}')(\lambda_0/\Delta x)/[64(\omega_i/\omega_r)^2 \times (1-n/n_c)]$, $K_{\nabla n}' = (1+v_d/c_s)^2(\Delta n/n_c)/(1-n/n_c)^{1/2}$, and $K_{\nabla v}' = 2(1+v_d/c_s)(\Delta v/c_s)(1-n/n_c)^{1/2}$, where v_d is the drift speed. Equation (1) is fitted (with $A = 0.025$) to a large number of kinetic simulations which studied Brillouin backscatter as a function of the parameters between the limits $0.3 < v_0/v_i < 2$, $10 < l/\lambda_0 < 252$, $0.05 < n/n_c < 0.7$, $1 < (T_e/T_i)_{\text{initial}} < 30$, and $(\omega_r/2\pi)t < 10$. Even in the short time and space scales of the kinetic simulations, there are very large oscillations (at fre-

quency $\sim \omega_r$) in the Poynting vector of the reflected and transmitted light.⁴ At times, much more light is reflected than is transmitted, since light undergoes multiple reflections even in an entirely underdense phase. Therefore we average over many $2\pi/\omega_r$. In the fluid model, inverse bremsstrahlung (IB) absorption also uses an exponential in space and so the Brillouin scattering and IB are numerically evaluated simultaneously in space and time by a sum of the arguments. The exponential model has the advantage that it is reasonably independent of zoning, and is suited to density and temperature gradients. Kruer's transcendental equation² showed a region of exponential increase with q for low q and a region of pump-depletion limit at high q , and consequently was zoning dependent if fitted to each zone. We model small reflection by modifying A so that total reflection from the previous time step agrees with Kruer's homogeneous transcendental equation² for space-integrated q . Equation (1) is reasonably good only for $v_0/v_i \lesssim 1$, and consequently the code has the nonlinear statement to describe wave saturation: $R/\lambda_0 \leq 0.08(n/n_c)(1-n/n_c)^{-1} \leq 0.17$ although kinetic simulations show that the saturation is more gradual and more complicated than this implies. At each time step, for each zone from vacuum to critical, starting with the edge that the laser first strikes, light is reflected according to Eq. (1). The ions are then heated according to the Manley-Rowe relations $\Delta T_i/\Delta t = R(\omega_r/\omega_0)(I/\ln i)$ and the intensity in the next zone away from the light is decreased by the fraction of light reflected by the previous zone.⁴ The ion heating increases the ion Landau damping which in turn can decrease the reflection on the next time step.⁴ Spherical expansion can cool the plasma.

Kinetic simulations with $0.05 \lesssim n/n_c \lesssim 0.25$ reveal that even underdense Raman scattering

heats in a surprisingly vigorous fashion and thus lowers q by increasing v_i and somewhat lowers the Raman T_{hot} by the ion fluctuations damping the electron plasma waves.³ Raman scattering would likely reduce the Brillouin scatter for the higher intensities of Fig. 1. The effects of a Raman model similar to the one in Fig. 1 will be given in a separate paper.

Brillouin scattering heats up the ions^{2,4} on each reflection and there can be multiple reflections.^{4,8} The model follows the light after one reflection from Brillouin scatter or critical density, after which the light may be absorbed, scattered again, or escape to vacuum. Kinetic simulations show that the ions are heated to a Maxwellian distribution of temperature $\approx (m_i/2)(\omega_r/k)^2$. Most of the heated ions are accelerated towards higher densities so that they are in position and velocity space to do the most damping. Since the ion-ion equilibration time is often not small, this effect

is significant. The heated-ion density n_{hot} is treated separately from the cold ions and self-consistently includes production and collisional equilibration to the cold-ion density. The total ion Landau damping is $\omega_i/\omega_r = (\omega_i/\omega_r)_{\text{hot}}(n_{\text{hot}}/n_{\text{tot}}) + (\omega_i/\omega_r)_{\text{cold}}(n_{\text{cold}}/n_{\text{tot}})$.

The model predicts absorption to better than 10% for most of a wide range of experiments (Fig. 1). Since unique experimental determination of Brillouin scatter is difficult to determine, the Brillouin-backscatter error bars could be greater than 10%. Since refraction, sidescatter, forward⁹ scatter, Raman heating and scatter, $2\omega_{pe}$ heating,¹⁰ rigorous noise frequency matching,^{6,7} IB reduction,¹¹ and ion turbulence absorption^{12,13} are not included, the experimental agreement is to some extent fortuitous. However, the scaling is interesting as a point of departure. One interesting point is that an increase in Brillouin scatter of $x\%$ generally decreases the absorption by much less than $x\%$. Since most of the Brillouin reflection often occurs at almost critical density, the IB and turbulence absorption are not too sensitive to Brillouin scattering, but of course the absorption at critical density is affected. Prepulse experiments by Amiranoff *et al.*¹⁴ show that the absorption for moderate-intensity pulses is not sensitive to prepulse although Brillouin backscatter is (as our model describes). The increased scale length from the prepulse both absorbs more by IB (less hot electrons) and scatters more. We used an approximation to Langdon's IB opacity¹¹ and found that greatly reduced Brillouin scatter would be necessary to match the experimental absorption. The evidence points to an additional absorption or electron-equilibration mechanism. Of course, in the 3D experiment, thermal conduction cools the spot (particularly the edges), which increases IB absorption. For filamentation to dominate^{10,15} Brillouin backscatter and sidescatter, $ZT_e/T_i \lesssim 1$ or the sideways gain q as determined by the plasma or spot width must be $\lesssim 10$.

What can be done about Brillouin scatter?

- (1) One can reduce the laser intensity.
- (2) One can increase or decrease the laser frequency (Fig. 1; see also Ref. 16). The dramatic increase in absorption for $\lambda_0 < 1 \mu\text{m}$ is primarily due to increased IB, which reduces Brillouin scatter by lowering v_0 and by increased competition.²

(3) One can use a multiline^{3,17} laser. If the difference between the frequencies is more than the Brillouin-backscatter growth rate γ , then

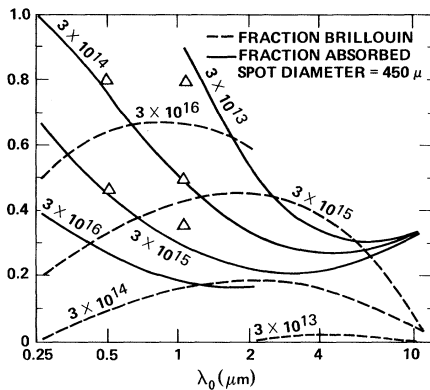


FIG. 1. Absorption (solid lines) and Brillouin reflection (dashed lines) predicted by LASNEX compared with experiments (Δ) with the intensity of the nearest solid line at that wavelength. Experiment and simulation were both on gold disks (Ref. 23). The spot sizes of the high-intensity and short-wavelength experiments were smaller than $450 \mu\text{m}$, but, for consistency, all the simulations had the same spot. The model reproduces the observed increase in Brillouin reflection as the spot size and/or the pulse length increases or the target \bar{z} decreases, since they will affect the number of Brillouin wavelengths and gradients. The absorption increases (Brillouin reflection decreases) (Ref. 2) for $\lambda_0 < 1 \mu\text{m}$ due primarily to increased inverse bremsstrahlung and lower v_0 . All the simulations assumed transport inhibition although this may not be true for lower $I\lambda_0^2$, in which case the model would predict more absorption. The internal Brillouin backscatter is greater than shown since some of the scattered light was absorbed on the way out.

the Brillouin scatter for each line is reasonably independent of the other and one can estimate the relative reduction in reflection by use of Eq. (1), by analyzing each line independently. Kinetic simulations (OREMP) have verified³ this method for two and seven lines. The Brillouin-backscatter growth rate γ is given by the following two limits^{12, 18} $\gamma/\omega_0 = (v_0/c)[(Zm_e/m_i)(n/n_c)(8c_s/c)^{-1}]^{1/2}$, $\gamma \ll kc_s$; and $\gamma/\omega_0 = 0.87[0.5(v_0/c)^2(Zm_e/m_i)(n/n_c)]^{1/3}$, $\gamma \gg kc_s$.

(4) One can increase the laser bandwidth ($\Delta\omega$), which essentially increases the gain length. There is experimental evidence^{16, 19} and theory^{3, 17} that bandwidth reduces the reflection due to Brillouin scattering (Fig. 2). For $\Delta\omega/\gamma$ greater than about 10, reflection is considerably reduced. The scaling $\Delta\omega/\gamma$ is simplified and Thomson¹⁷ has a more complete theoretical description. 2D kinetic simulations with $\Delta\omega = 0.1$ and 0 show about the same fraction of resonant absorption.²⁰

(5) One can reduce Brillouin sidescatter by about a factor of 2 (and also electron T_{hot}) by circular or cross polarization.

One can roughly estimate the Brillouin reflection for an experiment by simply assuming that the total damping is ~ 0.5 , and can consequently

simplify Eq. (1) to the following:

$$R \approx 1 - \exp[-0.05(v_0/v_t)^2(n/n_c)(l/\gamma_0)(1 - n/n_c)]^{-1},$$

where Raman scattering is ignored; $(v_0/v_t)^2 \approx [I(W/cm^2)/10^{16}][\lambda(\mu\text{m})]^2[4/T_e(\text{keV})]$, and to approximate saturation, one can say that if $v_0/v_t > 1.2$, it can be set equal to 1.2. For long pulses, the laser-target geometry has to be taken into account. If the geometry is Cartesian, then the spot size determines the density scale length, if that is smaller than $c_s t$. In spherical geometry, if l is longer than the pellet radius, spherical effects are clearly important. Also, if the light is obliquely incident, l is obviously greater than the density gradient length normal to the critical-density surface and is the ray trace path.

In measuring Brillouin scatter, it is important to consider²¹ that obliquely incident light may not come directly back towards the lens even with p polarization. An example from a fluid code¹⁵ with perpendicular incidence and s polarization shows the reflected light patterns in which about as much light is sidescattered as backscattered and is scattered and refracted to about a 45-deg angle relative to the normal for $v_0/v_t = 0.5$. Light sidescattered at high density is then refracted to a direction nearer to that of the density gradient. For sidescattering to be effective, the spot size must be typically $> 100\lambda_0$ wide, since many growth lengths in the sideways direction are needed and the plasma must be uniform and collisionless enough so that the light will not be lost by refraction to vacuum or absorption.

We suggest these reasons why laser-pellet interaction with 10- μm light²² has not shown much Brillouin reflection: (1) v_0/v_t is generally greater than 1, and so the ion wave amplitude is saturated. However, the time-averaged wave amplitude $\delta n/n$ is $\lesssim 0.5$, since the ion waves build up and crash. When they crash, the light transmits in that subsection. (2) The lower shelf density (n/n_c) is not very high. (3) Since the temperature is high and the density is low, $k\lambda_D$ can easily be > 1 , increasing ω_i/ω_r . (4) Since λ_0 is fairly long, l/λ_0 has not been large, but for many-nanosecond pulse lengths, l/λ_0 can be long enough for large reflection.

R. Berger (KMS Fusion), C. Randall (Lawrence Livermore Laboratory), D. Forslund (Los Alamos Scientific Laboratory), and W. Manheimer (Naval Research Laboratories) have recently reported computer and analytic models for Brillouin scatter.

We acknowledge many helpful conversations

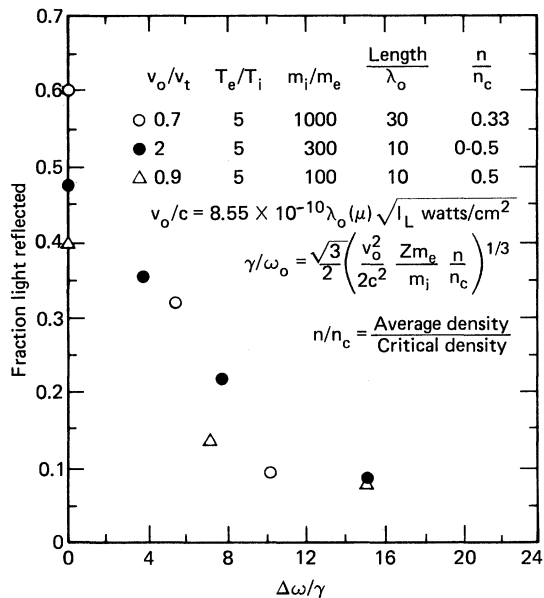


FIG. 2. Kinetic simulation results of reflection vs the ratio of the bandwidth of laser light to the growth rate of the Brillouin instability. This does not include inverse bremsstrahlung absorption, which would decrease Brillouin reflection even more with increasing $\Delta\omega$ or multilines since the absorption would decrease v_0/v_t .

with W. Kruer, C. Randall, V. Rupert, A. Langdon, B. Lasinski, C. Max, J. Thomson, G. McClellan, G. Caporaso, Y. Pan, D. Bailey, S. Bodner, and D. Biskamp. This work was performed under the auspices of the U. S. Department of Energy under Contract No. W-7405-ENG-448.

¹B. H. Ripin *et al.*, Phys. Rev. Lett. **39**, 611 (1977); B. Grek, H. Pépin, and F. Rheault, Phys. Rev. Lett. **38**, 898 (1977).

²D. W. Phillion, W. L. Kruer, and V. C. Rupert, Phys. Rev. Lett. **39**, 1529 (1977), and references within; W. L. Kruer, University of California Radiation Laboratory Report No. UCRL-50021-77, 1977 (unpublished), pp. 4-63.

³W. L. Kruer, K. G. Estabrook, and K. H. Sinz, Nucl. Fusion **13**, 952 (1973).

⁴Kent Estabrook, Bull. Am. Phys. Soc. **21**, 1067 (1976), and University of California Radiation Laboratory Report Nos. UCRL-50021-76, 1976 (unpublished), pp. 4-74, and UCRL-50021-78, 1978 (unpublished), pp. 3-63.

⁵B. D. Fried and R. W. Gould, Phys. Fluids **4**, 139 (1961). The complex integral equation describing ion Landau damping was solved for a large region of parameter space and then fitted to simple analytic formulas for the speed required in the fluid code.

⁶C. J. Randall *et al.*, Phys. Rev. Lett. **43**, 924 (1979); C. Randall *et al.*, University of California Radiation Laboratory Report No. UCRL-84330 (to be published).

⁷M. N. Rosenbluth, Phys. Rev. Lett. **29**, 565 (1972); K. Nishikawa and C. S. Liu, in *Advances in Plasma Physics*, edited by A. Simon and W. Thompson (Interscience, New York, 1976), Vol. 6, Eq. (III-58), where x has been replaced by the mismatch length as suggested by W. L. Kruer. This is only a rough approximation chosen from several ∇ models to give the best agreement with OREMP. A sharp (localized x) resonance reflects much less than OREMP, indicating that a broad resonance (noise) is needed. Of course, the experiment has noise that is different and probably greater than OREMP. G_{∇} has a minimum where $v_d = c_s$ and approximates a broad resonance.

⁸F. J. Mayer *et al.*, Phys. Rev. Lett. **44**, 1498 (1980).

⁹T. Johnston *et al.*, Bull. Am. Phys. Soc. **25**, 908 (1980).

¹⁰A. B. Langdon, B. F. Lasinski, and W. L. Kruer, Phys. Rev. Lett. **43**, 133 (1979); A. B. Langdon and B. F. Lasinski, Phys. Rev. Lett. **34**, 934 (1975); H. A. Baldis, J. C. Samson, and P. B. Corcum, Phys. Rev. Lett. **41**, 1719 (1978).

¹¹A. B. Langdon, Phys. Rev. Lett. **44**, 575 (1980).

¹²W. L. Kruer, unpublished, and private communication.

¹³R. L. Morse and C. W. Nielson, Phys. Rev. Lett. **26**, 3 (1971); W. M. Manheimer, Phys. Fluids **20**, 265 (1977); R. J. Faehl and W. L. Kruer, Phys. Fluids **20**, 55 (1977).

¹⁴F. Amiranoff *et al.*, J. Phys. (Paris), Colloq. **40**, C7-729 (1979); see also B. H. Ripin and E. A. McLean, Appl. Phys. Lett. **34**, 809 (1979).

¹⁵E. J. Valeo and K. G. Estabrook, Phys. Rev. Lett. **34**, 1008 (1975), and Phys. Fluids **19**, 1733 (1976).

¹⁶R. R. Johnson, P. M. Campbell, L. V. Powers, and D. C. Slater, in Proceedings of the Topical Meeting on Inertial Confinement Fusion, 7-9 February 1978, San Diego, California (unpublished); D. C. Slater and D. J. Tanner, in Proceedings of the Ninth Annual Conference on Anomalous Absorption of Electromagnetic Waves, 1979, Rochester, New York (unpublished).

¹⁷J. J. Thomson, Nucl. Fusion **15**, 237 (1975); G. Laval *et al.*, Phys. Fluids **20**, 2049 (1977).

¹⁸C. S. Liu *et al.*, Phys. Fluids **17**, 1211 (1974).

¹⁹C. Yamanaka *et al.*, Phys. Rev. Lett. **32**, 1038 (1974).

²⁰K. G. Estabrook, University of California Radiation Laboratory Report No. UCRL-81017, 1978 (unpublished); E. A. Williams and J. R. Albritton, in Proceedings of the Ninth Annual Conference on Anomalous Absorption of Electromagnetic Waves, Rochester, New York, 1979 (unpublished); T. Speziale, *ibid.*

²¹D. Biskamp and H. Welter, in *Plasma Physics and Controlled Nuclear Fusion Research-1974* (International Atomic Energy Agency, Vienna, 1975), Vol. II, p. 507; A. B. Langdon and B. F. Lasinski (private communication) have seen similar results.

²²D. W. Forslund, J. M. Kindel, E. L. Lindman, and K. Lee, private communication, and Phys. Fluids **18**, 1002, 1017 (1975).

²³M. D. Rosen *et al.*, Phys. Fluids **22**, 2020 (1979).